PROCEEDINGS OF SCIENCE

High precision measurement of the form factors of the semileptonic decays $K^{\pm} \to \pi^0 l^{\pm} \nu$ (Kl3) in NA48/2

Gianluca Lamanna[*†]
CERN
E-mail: gianluca.lamanna@cern.ch

The data collected by NA48/2 in 2003–2004 allowed several precise measurements in the charged kaon decay sector. In this paper we present the results obtained using a sample of 2.5×10^6 $K^{\pm} \to \pi^0 \mu^{\pm} \nu$ ($K_{\mu 3}$) and 4.0×10^6 $K^{\pm} \to \pi^0 l^{\pm} \nu$ (K_{e3}) events, collected in 2004 using a minimal trigger configuration. This unbiassed sample of kaon decays allows a high precision measurement of the semileptonic form factors.

Xth Quark Confinement and the Hadron Spectrum,
October 8-12, 2012
TUM Campus Garching, Munich, Germany

[*]Speaker.

[†]for the NA48/2 Collaboration: G. Anzivino, R. Arcidiacono, W. Baldini, S. Balev, J.R. Batley, M. Behler, S. Bifani, C. Biino, A. Bizzeti, B. Bloch-Devaux, G. Bocquet, N. Cabibbo, M. Calvetti, N. Cartiglia, A. Ceccucci, P. Cenci, C. Cerri, C. Cheshkov, J.B. Chèze, M. Clemencic, G. Collazuol, F. Costantini, A. Cotta Ramusino, D. Coward, D. Cundy, A. Dabrowski, P. Dalpiaz, C. Damiani, M. De Beer, J. Derré, H. Dibon, L. DiLella, N. Doble, K. Eppard, V. Falaleev, R. Fantechi, M. Fidecaro, L. Fiorini, M. Fiorini, T. Fonseca Martin, P.L. Frabetti, L. Gatignon, E. Gersabeck, A. Gianoli, S. Giudici, A. Gonidec, E. Goudzovski, S. Goy Lopez, M. Holder, P. Hristov, E. Iacopini, E. Imbergamo, M. Jeitler, G. Kalmus, V. Kekelidze, K. Kleinknecht, V. Kozhuharov, W. Kubischta, G. Lamanna, C. Lazzeroni, M. Lenti, L. Litov, D. Madigozhin, A. Maier, I. Mannelli, F. Marchetto, G. Marel, M. Markytan, P. Marouelli, M. Martini, L. Masetti, E. Mazzucato, A. Michetti, I. Mikulec, N. Molokanova, E. Monnier, U. Moosbrugger, C. Morales Morales, D.J. Munday, A. Nappi, G. Neuhofer, A. Norton, M. Patel, M. Pepe, A. Peters, F. Petrucci, M.C. Petrucci, B. Peyaud, M. Piccini, G. Pierazzini, I. Polenkevich, Yu. Potrebenikov, M. Raggi, B. Renk, P. Rubin, G. Ruggiero, M. Savrié, M. Scarpa, M. Shieh, M.W. Slater, M. Sozzi, S. Stoynev, E. Swallow, M. Szleper, M. Valdata-Nappi, B. Vallage, M. Velasco, M. Veltri, S. Venditti, M. Wache, H. Wahl, A. Walker, R. Wanke, L. Widhalm, A. Winhart, R. Winston, M.D. Wood, S.A. Wotton, A. Zinchenko, M. Ziolkowski.

PoS(Confinement X)243

1. Introduction

The semileptonic kaon decays provide the theoretically cleanest way to measure the CKM $|V_{us}|$ parameter and to perform the most accurate test of the CKM matrix unitarity. Departure of CKM unitarity in semileptonic kaon decays should be a clear signal of new physics [1], providing hints of different dynamics in the W-quark couplings. In addition, stringent constraints on new physics can be given by testing the lepton flavour universality [2].
The hadronic matrix element of the semileptonic kaon decays is usually described in terms of two dimensionless form factors $f_{\pm}(t)$, parametrized as a function of the squared four momentum transferred to the lepton system $t = (p_K - p_\pi)^2$:

$$M = \frac{G_F}{2} V_{us} (f_+(t)(p_K + p_\pi)^\mu \bar{u_l}\gamma_\mu(1+\gamma_5)u_\nu + f_-(t) m_l \bar{u_l}(1+\gamma_5)u_\nu) \; .$$

The function f_+ is related to the vector exchange (1^-) to the lepton system, while the function f_0, defined as

$$f_0(t) = f_+(t) + \frac{t}{m_K^2 - m_\pi^2} f_-(t) \; ,$$

is introduced to describe the scalar (0^+) exchange. Since the vector form factor at 0 momentum transferred can not be directly measured, the normalized form factors are defined as:

$$\bar{f_+}(t) = \frac{f_+(t)}{f_+(0)} \; , \; \bar{f_0}(t) = \frac{f_0(t)}{f_+(0)} \; .$$

Several parametrizations exist to describe the form factors. In this report we use the quadratic Taylor expansion and the pole parametrization. In the former case the normalized form factors are written as a function of the slope and curvature parameters $\lambda'_{+,0}$ and $\lambda''_{+,0}$:

$$\bar{f}_{+,0}(t) = 1 + \lambda'_{+,0} \frac{t}{m_\pi^2} + \frac{1}{2}\lambda''_{+,0} \left(\frac{t}{m_\pi^2}\right)^2 \; .$$

The disadvantage of such a parametrization is related to the strong correlations between the parameters and the absence of physical meaning of the λ parameters. In the pole parametrization this is avoided by applying physics constraints, reducing the number of parameters to the pole mass $M_{V,S}$ of a single resonance:

$$\bar{f}_{+,0}(t) = \frac{M_{V,S}^2}{M_{V,S}^2 - t} \; .$$

The results obtained with the quadratic fit can be related to a dispersive fit approach using the prescriptions given in [3].

2. The NA48/2 experiment

The NA48/2 experiment beam line was designed to measure the CP violating charged asymmetry in the $K \to 3\pi$ decay [4]. Simultaneous positive and negative kaon beams were produced by 400 GeV protons from the CERN/SPS accelerator impinging on a beryllium target. Particles of opposite charge with a central momentum of (60 ± 3) GeV/c were selected by two systems of

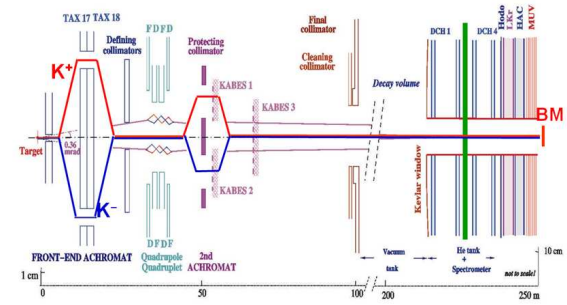

Figure 1: Layout of the NA48/2 charged kaon beam line.

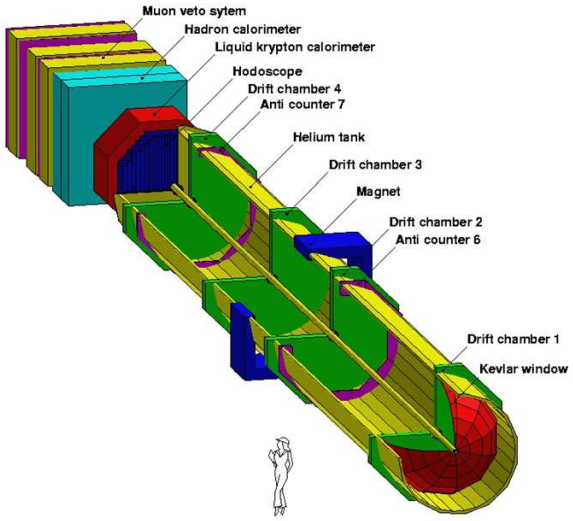

Figure 2: The NA48/2 downstream detectors.

dipole magnets ("achromats") and focused ~ 200 m downstream by a complex system of magnetic elements, at the end of the ~ 100 m long decay region. In fig.1 a schematic view of the beam line is shown. Both K^+ and K^- decays are collected concurrently in the NA48 detector (fig.2), described in full detail elsewhere [5]. The K_{l3} analysis is mostly based on:

- the magnetic spectrometer to measure the charged particle momentum, consisting of a magnet dipole with 120 MeV/c momentum kick and two sets of two drift chambers (DCH). Each chamber is made with 4 views (X,Y,U,V) of 2 wires planes. The final momentum resolution is $\sigma(p)/p = (1.02 \oplus 0.044 \cdot p)\%$ (p in GeV/c) and the position resolution is about $\sim 100 \mu m$.
- the electromagnetic calorimeter (LKr) to measure electromagnetic energy deposition of photons and electrons. The calorimeter has ~ 27 radiation lengths of liquid krypton and achieves an energy resolution $\sigma(E)/E = (3.2/\sqrt{E} \oplus 9.0/E \oplus 0.42)\%$ (E in GeV). It is used later to reconstruct $\pi^0 \to \gamma\gamma$ decays and identify electrons.
- the hodoscope (CHOD) to give a fast trigger signal for charged particle (the time resolution per track is $\sim 150 ps$). It consists of two orthogonal planes of scintillators segmented in horizontal and vertical slabs.
- the muon detector system (MUV) to identify muons in the $K_{\mu 3}$ selection. It consists of three segmented scintillator planes, each shielded by a 80 cm thick iron wall.

3. Event selection and background suppression

For both electron (K_{e3}) and muon ($K_{\mu 3}$) modes, a minimal trigger has been used to collect data in a dedicated run. It is based on one hit in the CHOD and an energy deposition greater than 10 GeV in the LKr. To select the decays, one track in the spectrometer and two clusters in the LKr are first requested. The track is then required to be in the detector acceptance with

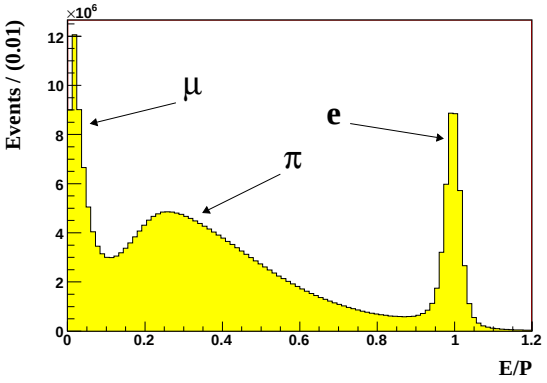

Figure 3: E/p distribution. Muons and electrons are distinguished using a cut on this variable.

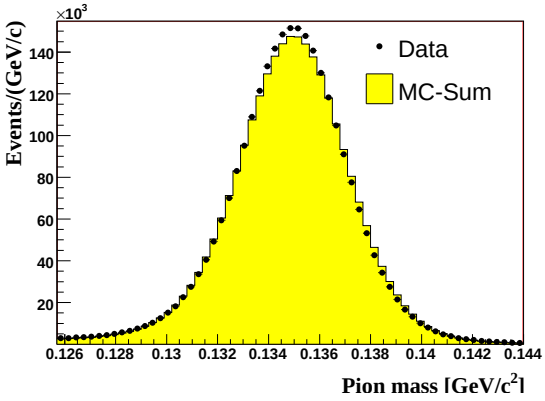

Figure 4: The $\gamma\gamma$ reconstructed mass is required to be close to the nominal π^0 mass.

a proper timing with respect to the trigger and the activity in the LKr. The momentum of the lepton is selected to be greater than 5 GeV/c for the electrons and greater than 10 GeV/c for the muons, to ensure full efficiency of the MUV system. The particle identification is based on the ratio of the visible energy in the electromagnetic calorimeter (E) and the measured momentum in the spectrometer (p). A charged track is identified as an electron if $0.95 < E/p < 1.05$ and has no associated hit in the MUV detector, while the muon identification requires $E/p < 0.2$ together with an associated hit in the MUV (fig.3). A cut on the $\gamma\gamma$ invariant mass, calculated assuming the vertex determined by the charged track and the kaon beam directions, is applied to select the π^0 decay: $|M_{\pi^0,PDG} - M_{\gamma\gamma}| < 10$ MeV/c^2 (fig.4). The total energy, reconstructed under the hypothesis of a single undetected neutrino, is required to be in the range $55 < E_{tot} < 65$ GeV , and the squared missing mass $(P_K - P_{\gamma\gamma} - P_{e,\mu})^2$ to be less than 10 (MeV/c^2)^2.

The background contribution is evaluated using a detailed GEANT3-based Monte Carlo simulation, including radiative corrections as described in [6]. The effect of these corrections was compared with a calculation obtained within Chiral Perturbation Theory with fully inclusive real photon emission [7]. The main background to the K_{e3} decay comes from the most frequent $K^\pm \to \pi^\pm\pi^0$ decay with a $\pi^\pm$ faking the electron. As shown in fig.5, a considerable background reduction is obtained by applying a cut on the electron transverse momentum $P_t > 0.02$ GeV/c. This cut reduces the signal acceptance by 3% and brings the background at the level of 0.1%. The $K^\pm \to \pi^\pm\pi^0$ decay is also the main background for the $K_{\mu 3}$ channel, due to the pion misidentification as a muon and the $\pi \to \mu\nu$ decay in flight. As shown in fig.6 a bi-dimensional cut in the (reconstructed kaon mass, π^0 transverse momentum) plane is applied to reduce the background contamination below 0.5%, at the price of a signal acceptance loss of $\sim$ 24%. The other background from $K \to \pi^\pm\pi^0\pi^0$ decay is subtracted from the data using the simulation. After these selection and background reduction cuts, we obtained a sample of about 2.5×10^6 $K_{\mu 3}$ and 4.0×10^6 K_{e3} candidates.

4. Dalitz plot fit procedure

A fit of the (E_l^*, E_π^*) Dalitz plot density is performed (E^* being the energies in the kaon rest frame) to extract the form factors. To improve the resolution of the Dalitz plot variables, the kaon

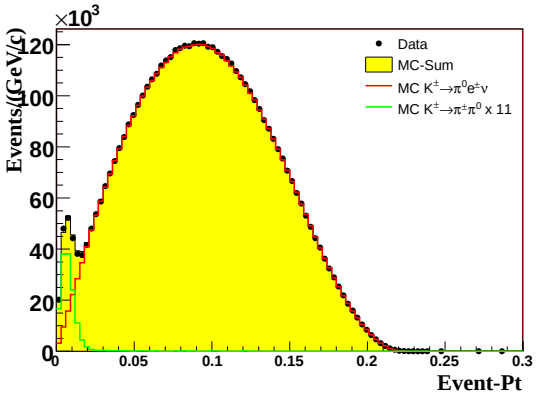

Figure 5: Transverse momentum distribution in K_{e3} selected events.The background contribution is clearly visible in the low Pt region.

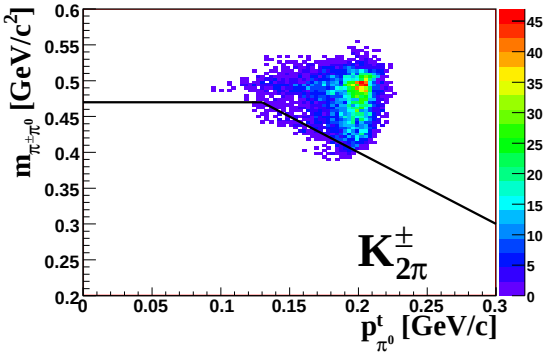

Figure 6: Two dimensional cut for $K_{\mu 3}$ events in the (π^0 transverse momentum, reconstructed $\pi^+\pi^0$ mass) plane.

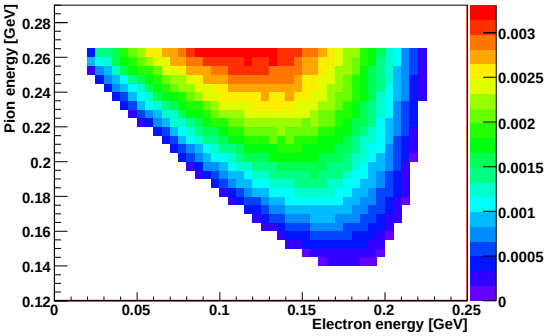

Figure 7: Dalitz plot distribution for selected K_{e3} events, after all corrections are applied.

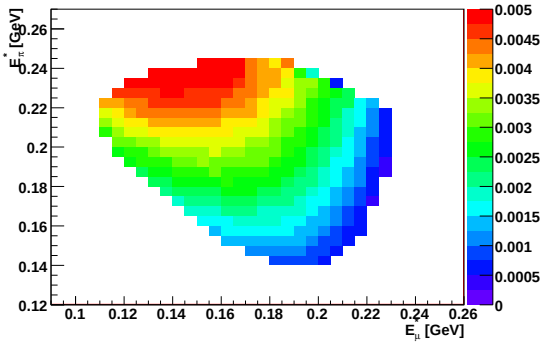

Figure 8: Dalitz plot distribution for selected $K_{\mu 3}$ events, after all corrections are applied.

energy is computed from the decay products under the assumption of a three-body decay with an undetected massless neutrino. This leads to two solutions for the longitudinal component of the kaon momentum, and the value closer to 60 GeV/c is used. The Dalitz Plot density is given by:

$$\rho(E_l^*, E_\pi^*) = \frac{d^2(E_l^*, E_\pi^*)}{dE_l^* dE_\pi^*} \propto A f_+^2(t) + B f_+(t)(f_0 - f_+)\frac{m_K^2 - m_\pi^2}{t} + C[(f_0 - f_+)\frac{m_K^2 - m_\pi^2}{t}]^2,$$

where A,B and C are known kinematical terms. The Dalitz Plot is subdivided in 5x5 MeV^2 bins. For each bin, acceptance, radiative effects and residual background subtraction are taken into account. The populated bins outside the physical region (due to resolution effects) are not considered for the fit (fig.7 and fig.8).

5. Results and conclusions

The preliminary results for both quadratic and pole parametrizations are summarized in table 5. The systematic uncertainties were evaluated by varying the selection cuts and the resolution of

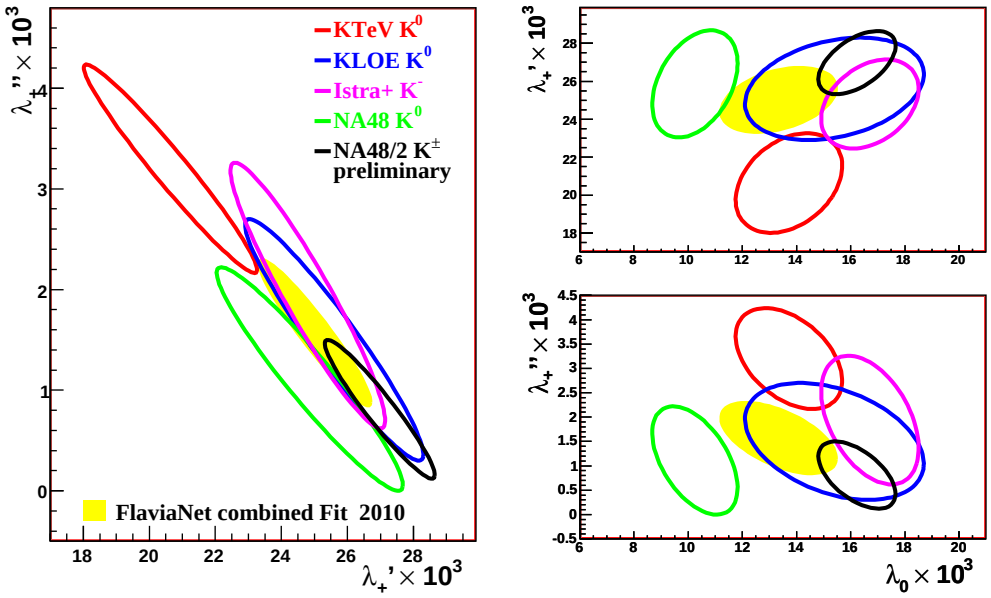

Figure 9: Comparison of the obtained results with the previous measurements of the λ parameters when combining the K_{e3} and the $K_{\mu 3}$ modes. All contours correspond to 68% confidence level fit results.

pion and muon energies in the kaon rest frame. In addition, the difference in the results between two independent analyses performed in parallel, was included in the systematic error. In tables 2 and 3 the contributions of both systematics and statistical errors are summarized. In the K_{e3} decay channel the systematics contribution is larger than the statistical one, while the $K_{\mu 3}$ error is dominated by the statistics. The good agreement between our result and the previous experiments [8] (except $K^0_{\mu 3}$ from NA48 [9]) is shown in fig.9 using 68% confidence level contours for the parameters λ of the Taylor expansion fit.

The average of the present results [10], together with additional experimental and theoretical inputs, allows to determine $|V_{us}| = (0.2254 \pm 0.0013)$. Using the best present value for $|V_{ud}|$ it is possible to estimate the departure from the unitarity for the CKM matrix: $\Delta_{CKM} = 0.0001 \pm 0.0006$. With a model-independent effective theory approach [11], it is possible to set the boundary to the scale for new physics contribution in the quark dynamics above 10 TeV.

In 2007, the NA62 experiment [2], using the same beam line as the NA48/2 experiment, collected a factor 10 more statistics with respect to the analysis presented here, both in K_{e3} and in $K_{\mu 3}$ modes. It collected also, in a special K_L run, $\sim 4 \times 10^6$ K^0_{e3} and $K^0_{\mu 3}$. The analysis of these data will help to further reduce the uncertainty on $|V_{us}|$.

References

[1] V. Bernard, M. Oertel, E. Passemar and J. Stern, Phys. Lett. B **638** (2006) 480 [hep-ph/0603202].

[2] C. Lazzeroni *et al.* [NA62 Collaboration], Phys. Lett. B **698** (2011) 105 [arXiv:1101.4805 [hep-ex]].

[3] V. Bernard, M. Oertel, E. Passemar and J. Stern, Phys. Rev. D **80** (2009) 034034 [arXiv:0903.1654 [hep-ph]].

[4] J. R. Batley *et al.* [NA48/2 Collaboration], Eur. Phys. J. C **52**, (2007) 875 [arXiv:0707.0697 [hep-ex]].

Quadratic ($\times 10^3$)	λ'_+	λ''_+	λ_0
$K^{\pm}_{\mu 3}$	$26.3 \pm 3.0_{stat} \pm 2.2_{syst}$	$1.2 \pm 1.1_{stat} \pm 1.1_{syst}$	$15.7 \pm 1.4_{stat} \pm 1.0_{syst}$
$K^{\pm}_{e3}$	$27.2 \pm 0.7_{stat} \pm 1.1_{syst}$	$0.7 \pm 0.3_{stat} \pm 0.4_{syst}$	
combined	27.0 ± 1.1	0.8 ± 0.5	16.2 ± 1.0
Pole (MeV/c^2)	m_V		m_S
$K^{\pm}_{\mu 3}$	$873 \pm 8_{stat} \pm 9_{syst}$		$1183 \pm 31_{stat} \pm 16_{syst}$
$K^{\pm}_{e3}$	$879 \pm 3_{stat} \pm 7_{syst}$		
combined	877 ± 6		1176 ± 31

Table 1: Preliminary results.

$K^{\pm}_{\mu 3}$	$\Delta\lambda'_+$	$\Delta\lambda''_+$ $\times 10^{-3}$	$\Delta\lambda_0$ MeV/c^2	Δm_V	Δm_S
Kaon energy	± 0.1	± 0.0	± 0.3	± 1	± 8
Vertex	± 1.0	± 0.5	± 0.1	± 2	± 7
Bin size	± 0.8	± 0.4	± 0.7	± 3	± 10
Energy scale	± 0.3	± 0.1	± 0.1	± 0	± 1
Acceptance	± 0.2	± 0.1	± 0.3	± 2	± 5
$K_{2\pi}$ background	± 1.7	± 0.5	± 0.6	± 3	± 0
2nd Analysis	± 0.1	± 0.1	± 0.2	± 2	± 5
FF input	± 0.3	± 0.8	± 0.1	± 7	± 3
Systematic	± 2.2	± 1.1	± 1.0	± 9	± 16
Statistical	± 3.0	± 1.1	± 1.4	± 8	± 31

Table 2: $K_{\mu 3}$ summary of systematics errors.

$K^{\pm}_{e3}$	$\Delta\lambda'_+$	$\Delta\lambda''_+$ $\times 10^{-3}$	Δm_V MeV/c^2
Kaon energy	± 0.3	± 0.1	± 6
Vertex	± 0.2	± 0.1	± 0
Bin size	± 0.0	± 0.1	± 2
Energy scale	± 0.1	± 0.0	± 0
Acceptance	± 0.2	± 0.0	± 3
2nd Analysis	± 0.9	± 0.4	± 1
FF input	± 0.4	± 0.0	± 7
Systematic	± 1.1	± 0.4	± 7
Statistical	± 0.7	± 0.3	± 3

Table 3: K_{e3} summary of systematics errors.

[5] V. Fanti *et al.* [NA48 Collaboration], Nucl. Instrum. Meth. A **574** (2007) 433.

[6] C. Gatti, Eur. Phys. J. C **45** (2006) 417 [hep-ph/0507280].

[7] V. Cirigliano, M. Giannotti and H. Neufeld, JHEP **0811** (2008) 006 [arXiv:0807.4507 [hep-ph]].

[8] M. Antonelli, V. Cirigliano, G. Isidori, F. Mescia, M. Moulson, H. Neufeld, E. Passemar and M. Palutan *et al.*, Eur. Phys. J. C **69** (2010) 399 [arXiv:1005.2323 [hep-ph]].

[9] A. Lai *et al.* [NA48 Collaboration], Phys. Lett. B **647** (2007) 341 [hep-ex/0703002].

[10] M. Moulson, arXiv:1209.3426 [hep-ex].

[11] V. Cirigliano, J. Jenkins and M. González-Alonso, Nucl. Phys. B **830** (2010) 95 [arXiv:0908.1754 [hep-ph]].